Finite Element Modeling of Electrical Machines by Simultaneous Resolution of Fields and Electric Circuits Equations

N. Sadowski*, R. Carlson*, J.P.A. Bastos*, M. Lajoie-Mazenc**

* GRUCAD-EEL-CTC-UFSC
C.P. 476
88040-900 - Florianópolis - SC - Brazil

** LEEI-ENSEEIHT-U.R.A. CNRS 847
2, Rue Camichel
31071 - Toulouse Cedex - France

Abstract **- In this work, we present a methodology for solving simultaneously the equations of magnetic fields and electric circuits of electrical machines. To consider the magnetic phenomena the Finite Element method is used. The machines are voltage fed and, thus, the electric circuit equations are present in the matricial system which takes into account both physical aspects. A time stepping technique is employed to simulate the steady and transient states. As result, we obtain the magnetic vector potential describing the magnetic behavior of the machine and the current established in the exciting coils.**

INTRODUCTION

The modeling of electrical machines and their feeding circuits is related to two type of equations: the Poisson equation describing their magnetic behavior and the differential equations of the electrical circuits related to the exciting windings.

It is also possible to determine the equivalent electrical circuit of the machine. By this procedure, it is necessary to obtain the parameters of the machine by analytical calculations or, for better accuracy, fields calculations. The equivalent electrical circuit, obtained by this procedure is associated to the electric feeding circuits [1],[2],[3]. This methodology presents limitations mainly when the machine has massive parts (not laminated regions), where eddy currents exist. In this case, it is practically impossible to determinate the equivalent electric circuit of the machine, for both, steady and transient states.

To solve such problems, it is necessary to solve simultaneously the field and circuit equations [4],[5],[6],[7],[8],[9],[10].

In this work, we present a brief survey based in works performed by us and, after the presentation of the general equations and solving techniques, the proposed methodology is illustrated by permanent magnet and induction motors fed by different electric circuits.

INVOLVED EQUATIONS

The global equations to solve are obtained associating the equation which describes the magnetic structure of the machine with the equations representing the feeding circuits.

Equations representing the magnetic structure of the machine

The general case of an electrical machine containing magnetic materials of reluctivity ν, permanent magnets with magnetization B_0 and reluctivity ν_p and with conductive solid parts with electrical conductivity σ is considered bellow.

If a two dimensional representation of the machine structure is adopted and using the magnetic vector potential A, the equations describing the whole structure are:

$$\frac{\partial}{\partial x}\left[\nu\frac{\partial A}{\partial x}\right]+\frac{\partial}{\partial y}\left[\nu\frac{\partial A}{\partial y}\right]-\sigma\frac{\partial A}{\partial t}+\frac{N}{S}I = \nu_p\left[\frac{\partial B_{0y}}{\partial x}-\frac{\partial B_{0x}}{\partial y}\right] \qquad (1.a)$$

$$U = RI + L\frac{dI}{dt}+\frac{N\ell}{S}\iint_S\frac{\partial A}{\partial t}ds \qquad (1.b)$$

where:
I is the current in the machine windings,
S is the winding surface,
N is the number of turns in the winding,
ℓ is the machine depth,
U is the voltage at the machine windings,
L represents the end winding inductance, not taken into account in a two dimensional magnetic representation of the machine.

The analytical solution of equations (1) is not easy to accomplish due to the complex structure of electrical machines. Then we adopt the Finite Element method [11]. Equations (1) can then be written in the following matrix form:

$$\mathbf{MA}+\mathbf{N}\frac{d}{dt}\mathbf{A}-\mathbf{PI}=\mathbf{D} \qquad (2.a)$$

$$\mathbf{Q}\frac{d}{dt}\mathbf{A}+\mathbf{RI}+\mathbf{L}\frac{d}{dt}\mathbf{I}=\mathbf{U} \qquad (2.b)$$

Matrices $\mathbf{M}, \mathbf{N}, \mathbf{P}, \mathbf{D}, \mathbf{Q}$ are dependent on the machine magnetic structure (dimensions, reluctivity,etc.).

Electrical feeding circuits equations

The differential equations representing the electric feeding circuits coupled to the machine windings can be written as:

$$\frac{d}{dt}\mathbf{X} = \mathbf{H_1X} + \mathbf{H_2E} + \mathbf{H_3I} \quad (3.a)$$

$$\mathbf{U} = \mathbf{H_4X} + \mathbf{H_5E} + \mathbf{H_6I} \quad (3.b)$$

where:
$\mathbf{X}$ is the inductance current and capacitor voltage vector of the electrical circuit connected to the machine,
$\mathbf{E}$ is the vector of the voltage sources of the external circuit,
matrices $\mathbf{H_1}, \mathbf{H_2}, \mathbf{H_3}, \mathbf{H_4}, \mathbf{H_5}, \mathbf{H_6}$ are dependent on the electrical circuit topology. Equation (3.b) allows coupling between magnetic and electric equations.

Global equations

Combining equations (2) and (3), the global matrix system representing the whole electrical machine-feeding circuit is obtained and given by (4). The unknowns in this global system are [5]:

a) the magnetic potential vector in the finite element mesh $\mathbf{A}$,
b) the currents in the machine windings $\mathbf{I}$,
c) the capacitor voltages and inductance currents in the feeding circuit (state variables).

$$\mathbf{MA} + \mathbf{N}\frac{d}{dt}\mathbf{A} - \mathbf{PI} = \mathbf{D} \quad (4.a)$$

$$\mathbf{Q}\frac{d}{dt}\mathbf{A} + [\mathbf{R} - \mathbf{H_6}]\mathbf{I} + \mathbf{L}\frac{d}{dt}\mathbf{I} - \mathbf{H_4X} = \mathbf{H_5E} \quad (4.b)$$

$$\frac{d}{dt}\mathbf{X} - \mathbf{H_1X} - \mathbf{H_3I} = \mathbf{H_2E} \quad (4.c)$$

Resolution Method

Equations (4) above are solved step by step with respect to time. In this way, the time derivatives must be discretized (by means of the θ-method or Euler's scheme [12]). During the step by step solution, the following must be observed:

a) The matrix terms concerning the external circuit can be modified due to the topologic changes in the feeding circuit (commutation of the semiconductors, for example).

b) Matrix $\mathbf{M}$ terms are modified due to the rotor movement.
c) If magnetic non-linearity must be taken into account an interactive procedure is used. In this work the Newton-Raphson method is employed [13].

The rotor movement is considered by remeshing the airgap at each position as follows.

Movement modeling

In this work, the movement is taken into account by a method based on meshing stator and rotor and connecting these meshes by an adaptable layer of Finite Elements placed in the air gap. This method is known as the Moving Band method. Its working principle is shown in Fig.1 [4],[10].

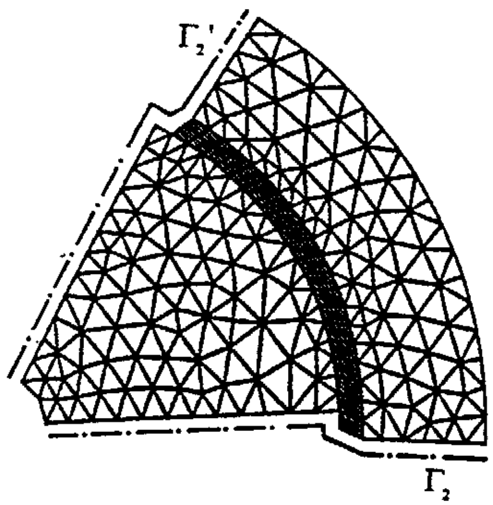

Fig. 1 : Moving Band method working principle.

According to the airgap deformation, the Moving Band technique is based in a dynamic allocation of the periodic or anti-periodic boundary conditions. With this technique, in spite of the new nodes created with the rotation of the moving part, the number of unknowns is always the same.

When using the Moving Band technique, if the rotation step is different than the discretization step, the finite elements placed in the airgap are deformed. This deformation can give rise to numerical oscillations on the voltages waveforms. To obtain better results, quadrilateral finite elements are used. These special elements are assembled in the global matrix as four triangular elements [10].

Torque calculation during the rotation

The choice of the method to simulate the rotor movement is related to the way employed to the torque calculation. This statement is based on studies made previously [10]. From this investigation, we concluded that the Maxwell Stress Tensor presents, with the Moving Band, very good accuracy. This method was chosen, but the following remark must be considered: if the displacement step is different of the discretization one (therefore, when there are deformations of the quadrilateral elements in the Moving Band), the torque is calculated in another layer of quadrilateral elements. This procedure is necessary to avoid numerical oscillations in the torque waveform.

APPLICATION EXAMPLES

We will present now two examples to describe the possibilities of the proposed method. These examples correspond to practical cases, which have been currently subjects of research.

Single phase line started induction motor fed by a starting circuit.

A two poles single phase induction motor used in electrical appliance applications is the first example. Its half structure as well as the calculated field distribution are shown in Fig.2 [14],[15]. In the same figure the induced current densities in the rotor bars at starting can be seen. The machine presents a different number of conductors by slot. Two windings are placed in the stator, namely the main and the auxiliary windings. A particular electric circuit shown in Fig. 3 is used to feed the machine. The resistance *R(t)* is time dependent.

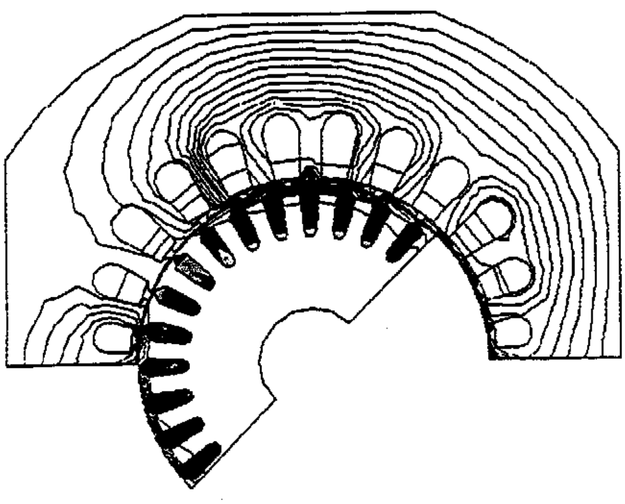

Fig. 2 : Single phase induction motor: field and induced current density distribution.

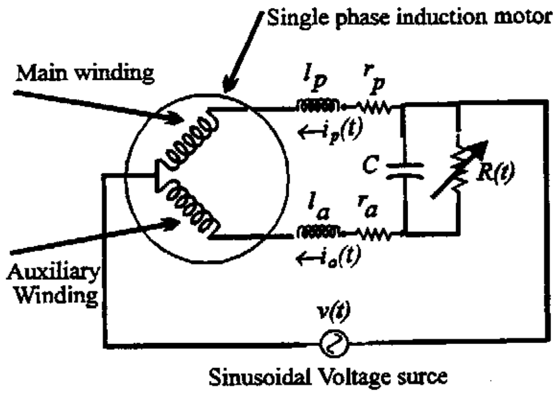

Fig. 3 : Single phase induction motor electrical feeding circuit.

Using electric circuits theory, matrices $\mathbf{H_1}, \mathbf{H_2}, \mathbf{H_3}, \mathbf{H_4}, \mathbf{H_5}, \mathbf{H_6}, \mathbf{L}$ and vector $\mathbf{E}$ associated to the electrical circuit of Fig. 3 can be obtained. Using Euler's scheme in order to represent the time derivatives in (4), one can write:

$$\mathbf{H_1} = \frac{-R(t)C - \Delta t}{R(t)C\Delta t} \quad (5.a) \qquad \mathbf{H_2} = 0 \quad (5.b)$$

$$\mathbf{H_3} = \begin{vmatrix} 0 & \frac{1}{C} \end{vmatrix} \quad (5.c) \qquad \mathbf{H_4} = \begin{vmatrix} 0 \\ -1 \end{vmatrix} \quad (5.d)$$

$$\mathbf{H_5} = \begin{vmatrix} 1 \\ 1 \end{vmatrix} \quad (5.e) \qquad \mathbf{H_6} = \begin{vmatrix} 0 & 0 \\ 0 & 0 \end{vmatrix} \quad (5.f)$$

$$\mathbf{R} = \begin{vmatrix} r_p & 0 \\ 0 & r_a \end{vmatrix} \quad (5.g) \qquad \mathbf{L} = \begin{vmatrix} l_p & 0 \\ 0 & l_a \end{vmatrix} \quad (5.h)$$

$$\mathbf{E} = v(t) \quad (5.i)$$

In equations (5) $v(t)$ is the applied voltage, r_p and r_a are the main and auxiliary winding d.c. resistances. The main and auxiliary end winding inductances are represented respectively by l_p and l_a. The $R(t)$ resistance and the capacitor C, already defined, are shown in Fig. 3. The time step is Δt.

In the simulation procedure, at each time step after the solution of equations (4), the electromagnetic torque Γ_e is calculated with the Maxwell Stress Tensor. The angular speed ω_m and the rotor displacement β are determinate with the following equations:

$$\frac{d\omega_m}{dt} = \frac{1}{J}\left[\Gamma_e - \Gamma_c - B\omega_m\right] \quad (6.a)$$

$$\frac{d\beta}{dt} = \omega_m \qquad (6.b)$$

where B is viscous damping factor, J is the inertia and Γ_c is the load torque.

Results: the simulation of the machine starting at no-load and fed by a 60 Hz sinusoidal voltage is presented in Figure 4. The resistance $R(t)$ has a small value in the beginning of the operation and it is strongly increased after 0.3 seconds. The effects of the resistance change can be noticed in the figures.

It is possible to remark the typical behavior of a single phase induction motor; the speed and current curves present particularly the oscillations having the double of the feeding frequency. In Figure 5 the calculated and experimental results at 670 rpm are presented. One can notice the good agreement between calculation and measurements.

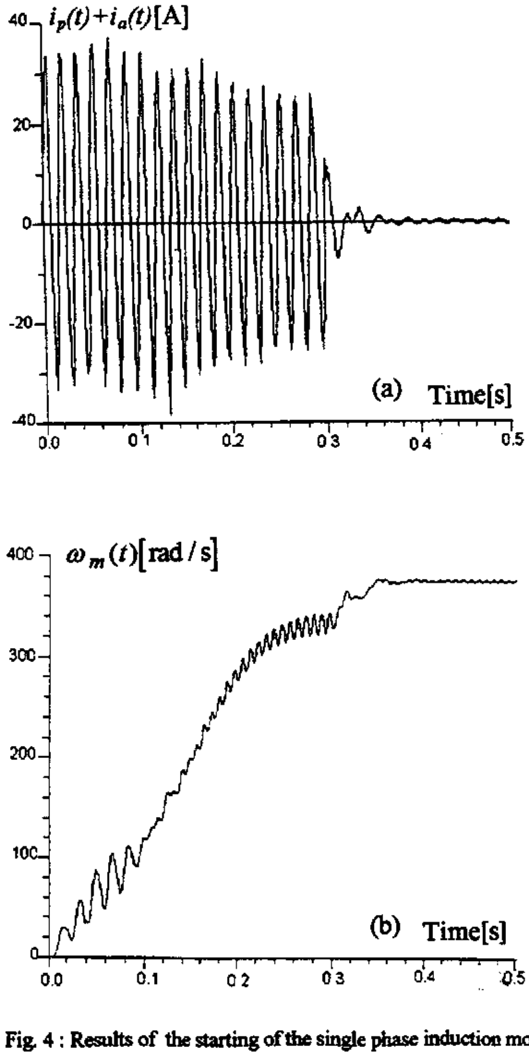

Fig. 4 : Results of the starting of the single phase induction motor. (a) Total (source) Current $i_p(t)+i_a(t)$. (b) Speed $\omega_m(t)$.

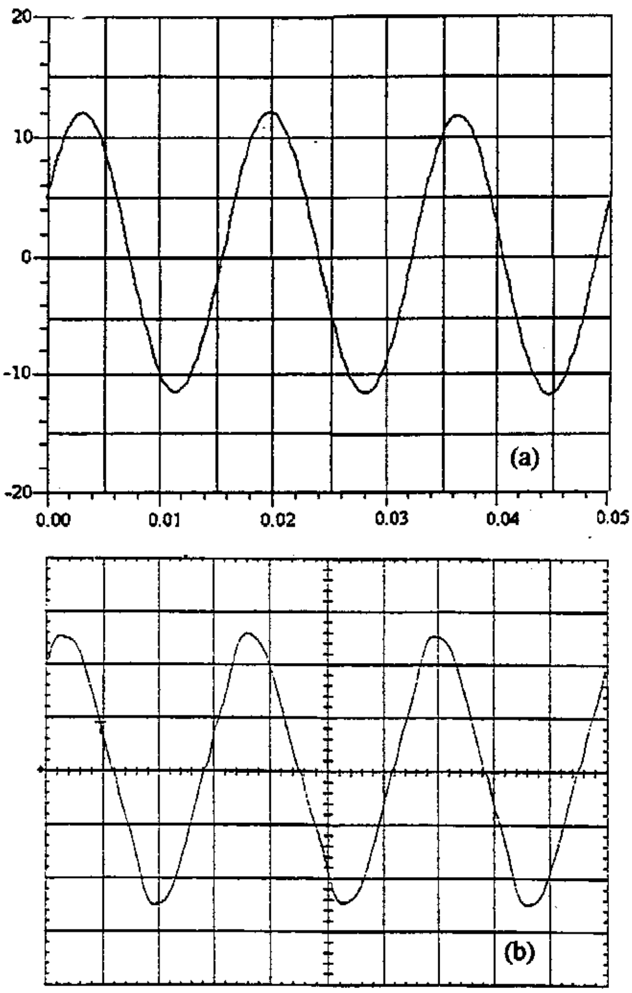

Fig. 5 :Total (source) Current $i_p(t)+i_a(t)$. (a) Calculated (5A/div.). (b) Experimental Results (5A/div.)

Permanent magnet motor fed by current inverter

The motor under study is fed by the inverter presented in Figure 6, in which there are thyristors connected to a current source, which is obtained by a voltage source connected to an inductance having a large value. The inverter is operated by a position sensor placed on the rotor.

To simulate such a device it is necessary to consider the actual structure of the electric circuit and its configuration changes due to the conducting states of the thyristors. Furthermore, the commutation of currents in the motor and the thyristor openings are made by the voltages in the motor terminals. Thus, the inverter operation and the machine are strongly associated and a simultaneous solution is the only procedure providing accurate results. In order to simplify the simulation, we take advantage of the fact

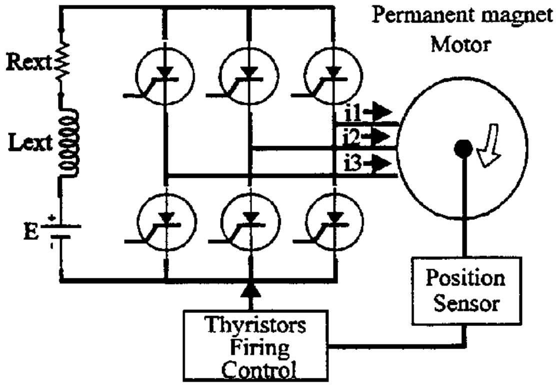

Fig. 6 : Current inverter working principle.

that the operation sequences of the inverter are known in advance and they can be described by only two sequences:

a) conduction, when two phases are fed and the third one is not connected.
b) commutation, when the three phases are connected and the voltage between two phases is zero.

These two states are successive and by circular permutation they describe the whole operation of the inverter. The electric circuits of these two sequences can be represent by the single circuit of Figure 7, where a resistance assuming values of 0 and 1 MΩ represents the respectively the commutation and the conducting sequences. This procedure allows us to keep constant the matricial system order.

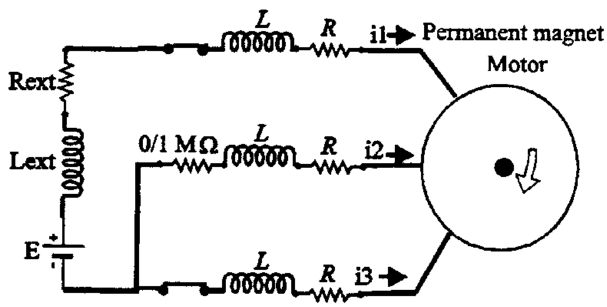

Fig. 7 : Circuit corresponding to the two working sequences.

The beginning of the commutation sequence is determinate by the position of the rotor. The end of this state occurs when the current in the commutation loop becomes zero. The motor shown in Fig. 8 was chosen for this example.

This machine presents permanent magnets in the rotor. They are mechanically sustained by an aluminum hoop and interpolar wedges, where eddy currents can be induced. Fig. 9 presents the eddy currents distribution during the motor operation.

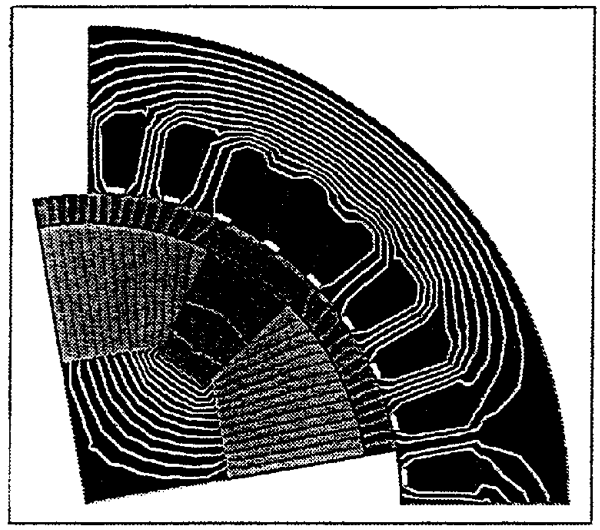

Fig. 8 : Permanent magnet structure domain.

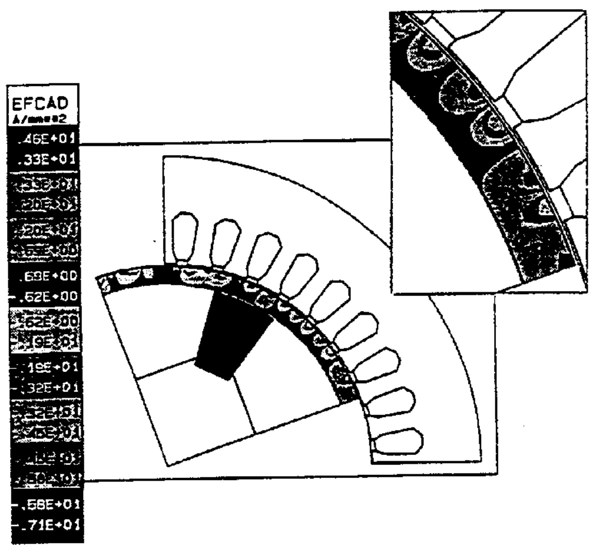

Fig. 9 : Eddy currents distribution in the conducting parts.

Figure 10 presents, using the same scales, the results obtained from the simulation and the experimental measurements. A very good agreement between these results is noticed. The eddy currents established in the aluminum hoop causes shorter commutation time, compared to the one expected for a device without induced currents.

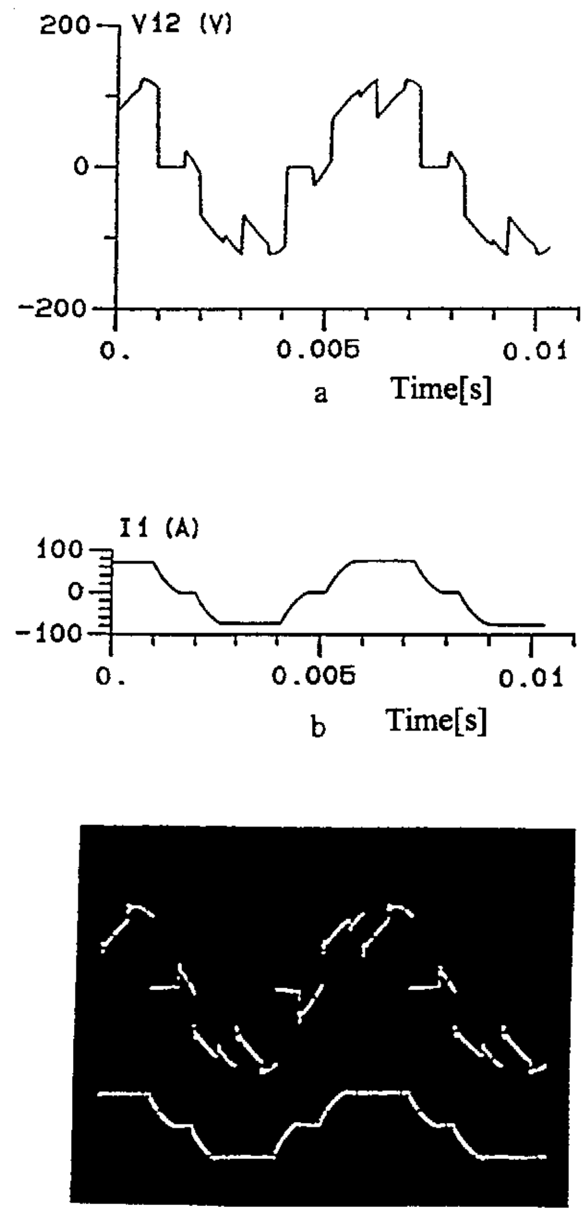

Fig. 10 : Voltage and currents of the inverter.

CONCLUSION

In this work a general modeling describing the functioning of the whole structure composed by a machine and its feeding circuit was presented. This procedure is based in the coupling between the magnetic field and the electric circuit equations.

When solving this system, the rotor movement was taken into account in the Finite Element geometric discretization of the domain. This technique is based on the concept of Moving Band using quadrilateral elements. The Maxwell Stress tensor is applied for torque calculation.

Two different simulation cases were presented: a single phase line started induction motor and a permanent magnet motor fed by a current inverter. For both cases, the calculated and the experimental results present a very good agreement.

Finally, when complex phenomena (eddy currents, non-linearity, movement and feeding by static converters) are present, the only method providing accurate results has to take into account simultaneously the different variables, as the one here proposed.

REFERENCES

[1] F.Piriou, A. Razek, "Calculation of saturated inductances for numerical simulation of synchronous machines", *IEEE Trans. on Magn.*, Vol. MAG-19, N.6, pp.2628-2631, November 1983.

[2] F. Piriou, A. Razek, "Modélisation des machines synchrones autopilotées en considérant la saturation magnétique", *Revue Générale d'Electricité*, Vol. 4, pp. 293-298, 1985.

[3] B. Davat, H. Rezine, M. Lajoie-Mazenc, "Modeling of a brushless DC motor with solid parts involving eddy currents", *IEEE Trans. on Industry Applications*, Vol. IA-21, N. 1, pp. 202-206, January/February 1985.

[4] Ren Z., *Contribution à la modélisation des machines électriques para résolution simultanée des équations du champ e des équations du circuit d'alimentation*, Thèse de Docteur de l'INPT, Toulouse, 1984.

[5] Davat B., *Modélisation des dispositifs électromagnétiques*, Thèse de Docteur ès-Sciences Physique, INPT, Toulouse, 1984.

[6] Arkkio, A., *Analysis of induction motors based on the numerical solution of the magnetic field and circuit equations*, Acta Polytechnica Scandinavica, Helsinki, 1987.

[7] F. Bouillault, A. Kladas, F. Piriou, A. Razek, "Coupled electric-magnetic model for a synchronous machine associated with static converter", Proceedings of ICEM, Pisa, pp. 453-456, 1988.

[8] Preston T.W., Reece A.B.J., Sangha P.S.,"Induction motor analysis by time-stepping techniques", *IEEE Trans. on Magn.*, Vol. 24, N.1, pp. 471-474, January 1988.

[9] Lombard P., Meunier G., "A general method for electric and magnetic coupled problems in 2D magnetodynamic domain", COMPUMAG Proceedings, Sorrento, pp. 195-198, July 1991.

[10] N. Sadowski, *Modélisation des machines électriques à partir de la résolution des équations du champ en tenant compte du mouvement et du circuit d'alimentation (Logiciel EFCAD)*, Thèse de Docteur de l'INPT, Toulouse, 1993.

[11] N. Ida, J.P.A.Bastos, *Electromagnetics and Calculation of Fields*, Springer-Verlag, New York, 1992.

[12] Raviart P.A., Thomas J.M., *Introduction à l'analyse numérique des équations aux dérivées partielles*, Masson, Paris, 1983.

[13] Silvester P.P., Chari M.V.K., "Finite element solution for saturable magnetic fields problems", *IEEE Trans. on Power Apparatus and Systems*, Vol. 89, pp. 1642-1651, 1970.

[14] N. Sadowski, R. Carlson, C.A. da Silva, L. Von Dokonal, "Simulation of Single Phase Induction Motors by Simultaneous Solution of Electrical and Field Equations", Proceedings of ICEM, Paris, 1994.

[15] N. Sadowski, R. Carlson, C. A. da Silva, M. Lajoie-Mazenc, "Simulation of Single Phase Induction Motor by a General Method for Coupling Field and Circuit Equations", Proceedings of IEEE-CEFC'94, Grenoble, 1994.

[16] N. Sadowski, B. Carly, Y. Lefevre, M. Lajoie-Mazenc, S. Astier, "Finite Element Simulation of Electrical Motors Fed by Current Inverters", *IEEE Trans. on Magn.*, Vol. 29, N. 2, March 1993, pp. 1683-1688.

[17] N. Sadowski, Y. Lefevre, M. Lajoie-Mazenc, J. Cros, "Finite Element Torque Calculation in Electrical Machines while Considering the Movement", *IEEE Trans. on Magn.*, Vol. 28, N. 2, March 1992, pp. 1410-1413.